SYNTHESIS OF THE NEW 2-ALKYL-*nido*-2,7,10-$C_3B_8H_{11}$ TRICARBABORANE BY PROTONATION OF [7-ALKYL-*nido*-7,8,10-$C_3B_8H_{10}$]$^-$: A REVERSIBLE CAGE-CARBON REARRANGEMENT

Alexandra M. SHEDLOW[1] and Larry G. SNEDDON[2,*]

Department of Chemistry, University of Pennsylvania, Philadelphia, Pennsylvania 19104-6323, U.S.A.; e-mail: [1] ashedlow@sas.upenn.edu, [2] lsneddon@sas.upenn.edu

Received January 30, 1999
Accepted February 27, 1999

Dedicated to Dr Stanislav Heřmánek on the occasion of his 70th birthday in recognition of both his outstanding contributions to the areas of borane chemistry and NMR spectroscopy, and his enthusiastic and encouraging support of the international community of boron researchers.

Protonation of the [7-R-*nido*-7,8,10-$C_3B_8H_{10}$]$^-$ (where R = $PhCH_2$ (**1a**) or R = Me (**1b**)) tricarbollide anion, with concentrated H_2SO_4 in a two-phase aqueous/CH_2Cl_2 system, yields the new neutral tricarbaborane: 2-R-*nido*-2,7,10-$C_3B_8H_{11}$ (where R = $PhCH_2$ (**2a**) or R = Me (**2b**)). The three cage-carbons of the [7-R-*nido*-7,8,10-$C_3B_8H_{10}$]$^-$ anion are located on the open face, but spectroscopic and DFT/GIAO/NMR studies of **2a** and **2b** show that during the protonation reaction, isomerization of the cage framework occurs to produce the neutral tricarbaborane having a 2,7,10-structure in which only two of the carbons remain on the open face. The third (R-substituted) carbon adopts a five-coordinate vertex off of the open face, thus enabling the incoming proton to adopt a bridging position on the B–B edge of the new C_2B_3-open face. The skeletal rearrangement is reversible, since deprotonation of **2a** or **2b** regenerates the anions **1a** and **1b**, respectively, having the 7,8,10-configuration. In agreement with the experimentally observed structures of the anionic (7,8,10-structure) and neutral (2,7,10-structure) species, DFT calculations at the B3LYP/6-311G*-level show that the [7-Me-*nido*-7,8,10-$C_3B_8H_{10}$]$^-$ anion (**1b**, structure **16**) is 28.9 kcal/mol more stable than the [2-Me-*nido*-2,7,10-$C_3B_8H_{10}$]$^-$ isomer (**3b**, structure **18**), while for the neutral tricarbaborane, the 2-R-*nido*-2,7,10-$C_3B_8H_{11}$ (**2b**, structure **14**) structure is more stable than any 7,8,10-structure (structures **7**–**11**) which has the added proton in an endo position on the open face. Transition state calculations at the HF/6-31G*-level yielded a simple, low-energy pathway (activation barrier of only 6.5 kcal/mol for the transition state **TS18/16**) for the rearrangement of [2-Me-*nido*-2,7,10-$C_3B_8H_{10}$]$^-$ (**3b**, structure **18**) to [7-Me-*nido*-7,8,10-$C_3B_8H_{10}$]$^-$ (**1b**, structure **16**) requiring the movement of only one cage atom, B11, from its original position in the C7–B8–B9–C10–B11 plane of **3b**, to the C7–C8–B9–C10–B11 plane of **1b**.

Key words: Boranes; Tricarbaboranes, Carboranes; Carbon rearrangement; DFT calculations; *Ab initio* calculations; GIAO calculations; NMR spectroscopy, ^1H, ^{13}C, ^{11}B.

The recent interest in tricarbaboranes has been stimulated by the development of efficient syntheses of both ten- and eleven-vertex tricarbaborane clusters[1–17]. For the eleven-vertex systems, two isomeric tricarbollide anions have been structurally characterized, [7-R-*nido*-7,8,9-$C_3B_8H_{10}$]$^-$ (**4**) and [7-R-*nido*-7,8,10-$C_3B_8H_{10}$]$^-$ (**1**) (Fig. 1, refs[6,9,11–14]).

Acidification of **4** (R = H) with CF_3CO_2H gave the parent tricarbaborane *nido*-7,8,9-$C_3B_8H_{12}$ (**5**) (Scheme 1) in which the added proton adopts a bridging position on the B10–B11 edge of the open face[9,14].

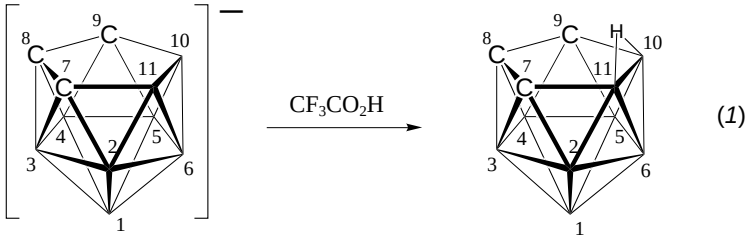

(*1*)

[*nido*-7,8,9-$C_3B_8H_{11}$]$^-$ **4** *nido*-7,8,9-$C_3B_8H_{12}$ **5**

SCHEME 1

The [7-R-*nido*-7,8,10-$C_3B_8H_{10}$]$^-$ isomer (**1**), however, lacks the open-face boron–boron edge that is needed to easily accommodate an additional proton. We report in this paper that reaction of [7-R-*nido*-7,8,10-$C_3B_8H_{10}$]$^-$ (where R = $PhCH_2$ (**1a**) and R = Me (**1b**)) with concentrated H_2SO_4 results in both protonation and cage isomerization to produce the new neutral tricarbaborane, 2-R-*nido*-2,7,10-$C_3B_8H_{11}$ (where R = $PhCH_2$ (**2a**) and R = Me (**2b**)) having a structure in which one of the cage carbons is no longer on

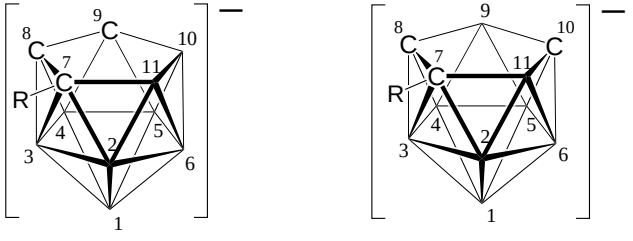

[7-R-*nido*-7,8,9-$C_3B_8H_{10}$]$^-$ **4** [7-R-*nido*-7,8,10-$C_3B_8H_{10}$]$^-$ **1**

FIG. 1

The two structurally characterized isomeric tricarbollide anions: [7-R-*nido*-7,8,9-$C_3B_8H_{10}$]$^-$ (**4**) (refs[9,11,14]) and [7-R-*nido*-7,8,10-$C_3B_8H_{10}$]$^-$ (**1**) (refs[6,12,14])

the open face. Furthermore, this skeletal rearrangement has been found to be reversible, since deprotonation of **2a** and **2b** regenerates **1a** and **1b**, respectively. DFT and HF *ab initio* calculations are presented that both establish the structures and relative energies of the neutral and anionic species and provide insight into the mechanism of the reversible isomerization reaction that interconverts their cage frameworks.

EXPERIMENTAL

All manipulations were carried out using standard high vacuum or inert-atmosphere techniques as described by Shriver[18].

Materials

The [7-R-*nido*-7,8,10-$C_3B_8H_{10}$]$^-$[PSH]$^+$ (where R = $PhCH_2$ (**1a**) and R = Me (**1b**)) were prepared according to literature methods[6]. The 1,8-bis(dimethylamino)naphthalene (Proton Sponge®, PS), diethyl ether, and heptane were purchased from Aldrich and used as received. Magnesium sulfate and sulfuric acid were purchased from Fisher Scientific and used as received. Methylene chloride was purchased from Aldrich and stored under N_2 until use.

Physical Measurements

^{11}B NMR spectra at 160.5 MHz, ^{1}H NMR spectra at 500.1 MHz, and ^{13}C NMR spectra at 125.7 MHz were obtained on a Bruker AMXII-500 spectrometer, equipped with the appropriate decoupling accessories. All ^{11}B chemical shifts are referenced to external $BF_3{\cdot}OEt_2$ (0.00 ppm) with a negative sign indicating an upfield shift. All ^{1}H and ^{13}C chemical shifts were measured relative to internal residual protons or carbons in CD_2Cl_2 and are referenced to Me_4Si (0.00 ppm). Two-dimensional COSY ^{11}B-^{11}B NMR and HETCOR ^{11}B-^{1}H experiments were performed at 160.5 MHz using the procedures described previously[19]. High- and low-resolution mass spectra were obtained on a VG-ZAB-E high-resolution mass spectrometer. Infrared spectra were obtained on a Perkin–Elmer 1430 spectrometer. Elemental analyses were performed at Robertson Microlit, Madison, NJ or the University of Pennsylvania microanalysis facility.

Reaction of [7-$PhCH_2$-*nido*-7,8,10-$C_3B_8H_{10}$]$^-$[PSH]$^+$ (**1a**) with Sulfuric Acid: Synthesis of 2-$PhCH_2$-*nido*-2,7,10-$C_3B_8H_{11}$ (**2a**)

A 50 ml, two-neck round-bottom flask fitted with vacuum stopcock was charged with [PSH]$^+$ **1a** (0.859 g, 1.95 mmol) dissolved in methylene chloride (10 ml). This solution was chilled in an ice water bath and 30 drops of concentrated H_2SO_4 were added slowly under a N_2 atmosphere. After 30 min, the methylene chloride layer was carefully decanted off. The sulfuric acid layer was washed with 1–2 ml CH_2Cl_2 and the methylene chloride layer was again carefully removed. All methylene chloride layers were collected, dried over $MgSO_4$, and filtered. The solvent was then vacuum evaporated leaving 0.342 g (1.51 mmol) of 2-$PhCH_2$-*nido*-2,7,10-$C_3B_8H_{11}$ (**2a**) as a white oily solid in a 77% unoptimized yield. IR (KBr, cm^{-1}): 3 050 (w), 3 010 (w), 3 002 (w), 2 950 (w), 2 920 (m), 2 550 (s), 1 630 (w), 1 582 (m), 1 573 (m), 1 440 (m), 1 410 (s), 1 370 (w), 1 260 (m), 1 235 (m), 1 200 (m), 1 175 (m), 1 162 (w),

1 100 (s), 1 090 (m), 1 060 (m), 1 035 (m), 1 015 (m), 980 (m), 947 (m), 840 (m), 790 (w), 730 (w). HRMS (*m/z*) calculated for $^{12}C_{10}{}^{1}H_{18}{}^{11}B_8$ (P): 226.2153; found: 226.2150. Analysis: for $C_{10}H_{18}B_8$ (224.7) (**2a**) calculated: 53.45% C, 8.07% H; found: 54.56% C, 7.98% H.

Reaction of [7-Me-*nido*-7,8,10-$C_3B_8H_{10}]^-[PSH]^+$ (**1b**) with Sulfuric Acid: Synthesis of 2-Me-*nido*-2,7,10-$C_3B_8H_{11}$ (**2b**)

In a manner similar to that above, $[PSH]^+$ **1b** (0.711 g, 1.95 mmol) dissolved in methylene chloride (10 ml) was chilled in an ice water bath, and reacted with 30 drops of concentrated H_2SO_4 for 30 min under a N_2 atmosphere. The methylene chloride layer was then carefully decanted off. The sulfuric acid layer was washed with 1–2 ml CH_2Cl_2 and the methylene chloride layer was again carefully removed. All methylene chloride layers were collected, dried over $MgSO_4$, and filtered. The solvent was vacuum evaporated leaving a white oily solid identified as 2-Me-*nido*-2,7,10-$C_3B_8H_{11}$ (**2b**) (0.275 g, 1.83 mmol, 94% yield). IR (KBr, cm^{-1}): 3 045 (w), 3 007 (m), 2 980 (s), 2 960 (s), 2 920 (w), 2 580 (m), 2 520 (m), 1 610 (w), 1 592 (w), 1 457 (m), 1 421 (s), 1 372 (m), 1 315 (m), 1 301 (m), 1 258 (m), 1 225 (m), 1 180 (m), 1 090 (w), 1 010 (w), 982 (m), 928 (w), 831 (w), 760 (w). HRMS (*m/z*) calculated for $^{12}C_4{}^{1}H_{14}{}^{11}B_8$ (P): 150.1839; found: 150.1840. Analysis: for $C_4H_{14}B_8$ (148.6) (**2b**) calculated: 32.32% C, 9.49% H; found: 32.28% C, 9.41% H.

Reaction of **2a** with PS: Synthesis of $[PSH]^+$[7-$PhCH_2$-*nido*-7,8,10-$C_3B_8H_{10}]^-$ ($[PSH]^+$**1a**)

A 50 ml two-neck round-bottom flask fitted with a vacuum stopcock was charged with **2a** (0.342 g, 1.51 mmol) which was then dissolved in methylene chloride (15 ml) under a N_2 atmosphere. To this stirred solution was added PS (0.323 g, 1.51 mmol). After 20 min, the solvent was vacuum evaporated, the solid was recrystallized using a methylene chloride–diethyl ether–heptane mixture to give a pale yellow solid which was identified on the basis of its ^{11}B and ^{1}H NMR spectra as the known salt[6] $[PSH]^+$[7-$PhCH_2$-*nido*-7,8,10-$C_3B_8H_{10}]^-$ ($[PSH]^+$**1a**) (0.645 g, 1.46 mmol, 97% yield).

Reaction of **2b** with PS: Synthesis of $[PSH]^+$[7-Me-*nido*-7,8,10-$C_3B_8H_{10}]^-$ ($[PSH]^+$**1b**)

A 0.275 g (1.83 mmol) sample of 2-Me-*nido*-2,7,10-$C_3B_8H_{11}$ (**2b**) was dissolved in methylene chloride (15 ml) under a N_2 atmosphere. To this stirred solution was added PS (0.392 g, 1.83 mmol). After 20 min, the solvent was vacuum evaporated, the solid was recrystallized using a methylene chloride–diethyl ether–heptane mixture to yield 0.652 g (1.79 mmol, 98% yield) of a pale yellow solid which was identified on the basis of its ^{11}B and ^{1}H NMR spectra as the known salt[6] $[PSH]^+$[7-Me-*nido*-7,8,10-$C_3B_8H_{10}]^-$ ($[PSH]^+$**1b**).

Computational Methods

The DFT/GIAO/NMR method[20], using the GAUSSIAN94 program[21], was used in a manner similar to that previously described[22]. The geometries were first fully optimized at the HF/6-31G* level and then at the DFT B3LYP/6-311G* level within the specified symmetry constraints (using the standard basis sets included) on a two-processor Origin 2000 computer running IRIX 6.4. Calculations that would include the benzyl exo-polyhedral substituent were not possible, since such calculations would be too large for our available computational resources. Thus, only methyl or hydrogen substituted derivatives were em-

ployed for the calculations. A vibrational frequency analysis was carried out on each optimized geometry (non-transition state) at the HF/6-31G* and the DFT B3LYP/6-311G* levels with a true minimum found for each structure (*i.e.* possessing no imaginary frequencies). The NMR chemical shifts were calculated using the GIAO option within GAUSSIAN94 at the B3LYP/6-311G*//B3LYP/6-311G* optimization level. ^{11}B NMR GIAO chemical shifts were referenced to $BF_3{\cdot}OEt_2$ using an absolute shielding constant of 102.24 ppm (refs[23,24]). ^{13}C NMR GIAO chemical shifts were referenced to TMS using an absolute shielding constant of 184.38 ppm. Tables of cartesian coordinates and selected bond distances and angles of the optimized geometries are available from the authors.

For the reaction pathway transition state calculations, all geometries were optimized at the HF/6-31G* level, since MP2/6-31G* level calculations were too large for the available computational resources[25]. Vibrational frequencies were calculated at the same level to determine the nature of the stationary point and to make zero-point corrections. The stationary point was judged to be a true transition state possessing one imaginary frequency of magnitude i289 cm^{-1}. An IRC calculation was done to confirm the reaction pathway in both directions from the located transition state.

RESULTS AND DISCUSSION

We previously reported the synthesis of the [7-R-*nido*-7,8,10-$C_3B_8H_{10}$]$^-$ tricarbollides (where R = $PhCH_2$ (**1a**, 56%) and R = Me (**1b**, 61%)) by a cage expansion route involving the reaction of [6-R-*nido*-5,6,9-$C_3B_7H_9$]$^-$ (**6**) with $BrBH_2{\cdot}SMe_2$, accompanied by *in situ* deprotonation with proton sponge (Scheme 2, ref.[6]).

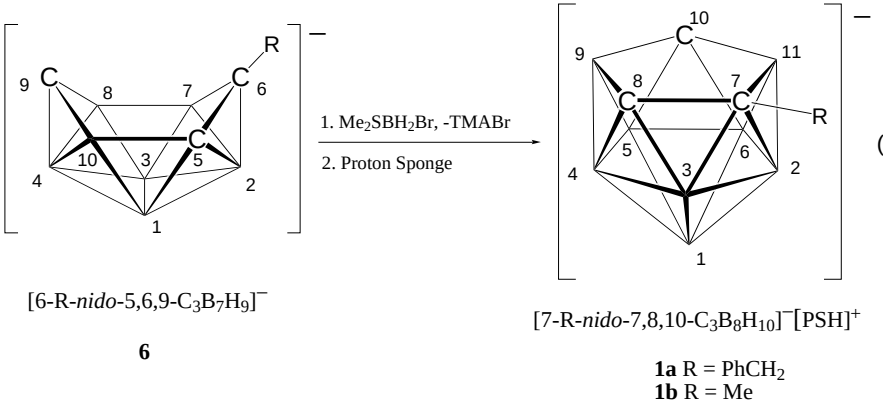

[6-R-*nido*-5,6,9-$C_3B_7H_9$]$^-$

6

[7-R-*nido*-7,8,10-$C_3B_8H_{10}$]$^-$[PSH]$^+$

1a R = $PhCH_2$
1b R = Me

SCHEME 2

An X-ray structural determination of **1a** and *ab initio*/IGLO computational studies (HF/6-31G*-level) on **1b** confirmed an eleven-vertex *nido* cage-geometry for these anions having a five-membered C_3B_2-open face, with the two borons in non-adjacent positions.

We have now found that, while both **1a** and **1b** are remarkably unreactive toward most electrophiles, they are readily protonated upon reaction with concentrated H_2SO_4 to form the neutral tricarbaboranes 2-$PhCH_2$-*nido*-2,7,10-$C_3B_8H_{11}$ (**2a**) (≈77% yield) and 2-Me-*nido*-2,7,10-$C_3B_8H_{11}$ (**2b**) (≈94% yield), respectively (Scheme 3). The two compounds were isolated in pure form as oily solids and their proposed compositions are supported by both microanalytical and exact mass determinations.

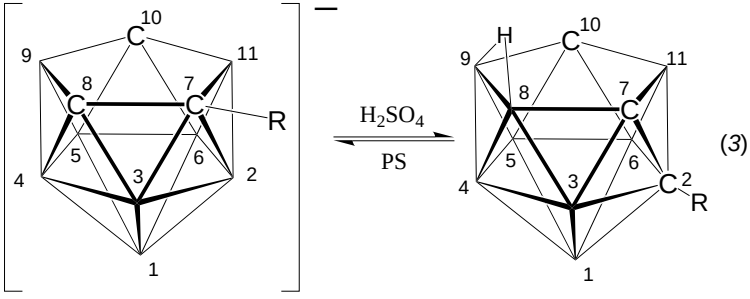

[7-R-*nido*-7,8,10-$C_3B_8H_{10}$]$^-$[PSH]$^+$
R = $PhCH_2$ (**1a**); Me (**1b**)

2-R-*nido*-2,7,10-$C_3B_8H_{11}$
R = $PhCH_2$ (**2a**); Me (**2b**)

SCHEME 3

The ^{11}B NMR spectra of the two tricarbaboranes are almost identical, each showing 8 doublet resonances indicative of C_1 symmetry (Table I). No evidence for fluxional behavior was seen in the low-temperature ^{11}B NMR spectra of either **2a** or **2b**. As can be seen in the ^{11}B NMR spectrum of **2b** shown in Fig. 2, the resonances near –18 and –21 ppm in the spectra of both **2a** and **2b** show fine-structure (J_{BH} ≈ 50 Hz) characteristic of bridge- hydrogen coupling.

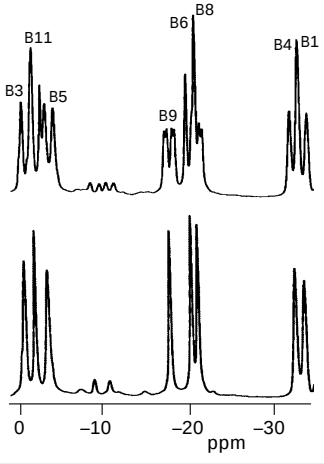

FIG. 2
160.5 MHz ^{11}B NMR spectra of 2-Me-*nido*-2,7,10-$C_3B_8H_{11}$ (**2b**): ^1H-coupled (top), ^1H-decoupled (bottom)

Supporting this conclusion, the ^{1}H NMR spectrum of each compound shows, in addition to the resonances expected for the two cage-CH protons and the benzyl (**2a**) and methyl (**2b**) groups, a single broad resonance, at –1.61 ppm for **2a** and –1.67 ppm for **2b**, in the upfield region expected for a bridge-hydrogen. For **2b**, this broad peak shows a septet coupling-pattern, with the 1 : 2 : 3 : 4 : 3 : 2 : 1 ratios characteristic of a bridge-hydrogen cou-

TABLE I
Experimental NMR data (δ in ppm)

Compound	Nucleus	δ (multiplicity, assigment, *J* (Hz))
2a	^{11}B[a,b]	–1.8 (d, B3, *J*(B,H) = 182); –3.0 (d, B11, *J*(B,H) = 160); –4.0 (d, B5, *J*(B,H) ≈ 160); –17.4 (d, B9, *J*(B,H) = 140, *J*(B,μ-H) = 48); –21.3 (d, B6, *J*(B,H) ≈ 150); –21.7 (d, B8, *J*(B,H) ≈ 155); –33.7 (d, B4, *J*(B,H) = 148); –34.7 (d, B1, *J*(B,H) = 167)
	^{11}B-^{11}B[a,b]	observed crosspeaks: B1-B3, –B4, –B5; B3-B4, –B8; B4-B5, –B8, –B9; B5-B6. Missing: B5-B9; B6-B11; B8-B9
	^{1}H[b,c]	8.2–7.1 (m, Ph); 3.24 (s, CH_2); 2.97 (1, BH); 2.62 (1, BH); 2.23 (1, BH); 1.96 (1, CH); 1.85 (1, CH); 1.55 (1, BH); 1.21 (1, BH); 0.89 (1, BH); 0.61 (1, BH); 0.32 (1, BH); –1.61 (1, BHB)
	^{1}H-^{11}B[a,b,c]	selected observed crosspeaks: μ-H(–1.61 ppm)-B9(–17.4 ppm); μ-H(–1.61 ppm)-B8(–21.7 ppm)
	^{13}C{^{1}H} (–60 °C)[b,d,e]	135.9–127.2 (m, Ph); 57.8 (s, C2); 41.2 (s, CH_2); 36.8 (s, br, C10); 33.0 (s, br, C7)
2b	^{11}B[a,b]	–0.73 (d, B3, *J*(B,H) = 202); –2.0 (d, B11, *J*(B,H) = 162); –3.5 (d, B5, *J*(B,H) = 162); –18.0 (d, B9, *J*(B,H) = 143, *J*(B,μ-H) = 47); –20.5 (d, B6, *J*(B,H) = 170); –21.3 (d, B8, *J*(B,H) = 112, *J*(B,μ-H) = 52); –32.9 (d, B4, *J*(B,H) = 157); –34.0 (d, B1, *J*(B,H) = 178)
	^{11}B-^{11}B[a,b]	observed crosspeaks: B1-B3, –B4, –B5; B3-B4, –B8; B4-B5, –B8, –B9; B5-B6. Missing: B5-B9; B6-B11; B8-B9
	^{1}H[b,c]	1.99 (1, CH); 1.87 (1, CH); 1.72 (s, CH_3); –1.67 (m, BHB, *J*(μ-H,B) = 48)
	^{1}H{^{11}B}[a,b,c]	2.96 (2, BH); 2.57 (2, BH); 2.47 (1, BH); 1.99 (1, CH); 1.95 (1, BH); 1.87 (1, CH); 1.72 (s, CH_3); 1.50 (1, BH); 0.77 (1, BH); –1.67 (s, BHB)
	^{13}C[b,f]	41.4 (d, C7, *J*(C,H) = 173); 34.9 (d, C10, *J*(C,H) = 168); 24.0 (q, C2a, *J*(C,H) = 132)
	^{13}C (–83 °C)[b,f]	61.6 (s, C2); 40.0 (d, C7, *J*(C,H) = 163); 33.8 (d, C10, *J*(C,H) = 169); 23.3 (q, C2a, *J*(C,H) = 132)

[a] 160.5 MHz; [b] CD_2Cl_2; [c] 500.1 MHz; [d] 50.3 MHz; [e] solubility problems prevented lower temperatures; [f] 125.7 MHz.

pled to two ^{11}B atoms (I = 3/2). Additional 2D ^{11}B-^{1}H HETCOR experiments on both **2a** and **2b** also confirmed coupling between the upfield proton resonances and the –18 and –21 ppm resonances in the ^{11}B NMR spectra. The resonances at –1.61 and –1.67 ppm collapse to sharp singlets in the $^{1}H\{^{11}B\}$ NMR spectra. The ^{13}C NMR spectrum of each compound at –83 °C shows two broad doublets (cage-CH resonances) and a singlet (cage-CR), along with the carbon-resonances of the exo-polyhedral substituents (**2a**, $PhCH_2$; **2b**, Me).

Attempts to grow X-ray quality crystals of **2a** or **2b** were not successful; therefore, DFT/GIAO/NMR calculations were employed to confirm their structures.

Unlike the 7,8,9-tricarbollide anion (**4**), the 7,8,10-tricarbollide anion, (**1a** and **1b**), does not have a B–B edge on the five-membered open face to

TABLE II
Comparison of the experimental ^{11}B and ^{13}C NMR chemical shifts and assignments of 2-Me-*nido*-2,7,10-$C_3B_8H_{11}$ (**2b**) with the calculated[a] shifts and assignments of 7-Me-7,8,10-structures, **7**–**11**, containing endo-hydrogens (structures shown in Fig. 3)

2b Experimental	**7** Calculated	**8** Calculated	**9** Calculated	**10** Calculated	**11** Calculated
			^{11}B NMR shifts		
0.73 (B3)	–4.2 (B11)	6.4 (B5)	12.8 (B3)	13.1 (B3)	7.8 (B6)
–2.0 (B11)	–4.7 (B9)	4.7 (B2)	0.57 (B9)	1.7 (B11)	0.55 (B4)
–3.5 (B5)	–4.9 (B3)	–2.9 (B11)	–4.4 (B6)	–6.6 (B5)	–0.27 (B2)
–18.0 (B9)	–15.2 (B6)	–3.1 (B4)	–12.8 (B11)	–9.9 (B9)	–5.4 (B9)
–20.5 (B6)	–17.1 (B5)	–14.7 (B3)	–13.8 (B5)	–10.0 (B6)	–12.2 (B3)
–21.3 (B8)	–19.0 (B2)	–18.4 (B6)	–16.7 (B4)	–14.1 (B2)	–20.5 (B5)
–32.9 (B4)	–22.6 (B4)	–19.2 (B1)	–31.0 (B1)	–30.8 (B1)	–20.8 (B1)
–34.0 (B1)	–36.9 (B1)	–38.6 (B9)	–31.9 (B2)	–32.8 (B4)	–34.3 (B11)
			^{13}C NMR shifts		
61.6 (C2)	65.76 (C7)	88.48 (C8)	49.14 (C10)	53.74 (C7)	106.25 (C7)
40.0 (C7)	55.18 (C8)	77.39 (C7)	48.38 (C7)	48.86 (C10)	72.19 (C10)
33.8 (C10)	24.48 (C7a)	74.90 (C10)	48.25 (C8)	28.22 (C8)	66.10 (C8)
23.3 (C2a)	12.37 (C10)	24.88 (C7a)	22.74 (C7a)	24.13 (C7a)	26.78 (C7a)

[a] Calculations at the DFT B3LYP/6-311G*//B3LYP/6-311G* level.

accommodate a bridge hydrogen. Thus, if protonation of **1a** and **1b** were to occur on the 7,8,10-C_3B_2-face of the anion, then the proton would have to adopt an endo position on one of the five atoms on the face. Optimized geometries (**7**–**11**) at the DFT B3LYP/6-311G* level were, in fact, found for protonation at the endo position of all cage atoms (Fig. 3). However, the GIAO calculated ^{11}B and ^{13}C chemical shifts and assignments for these structures do not agree with those experimentally determined for **2a** and **2b** (Table II).

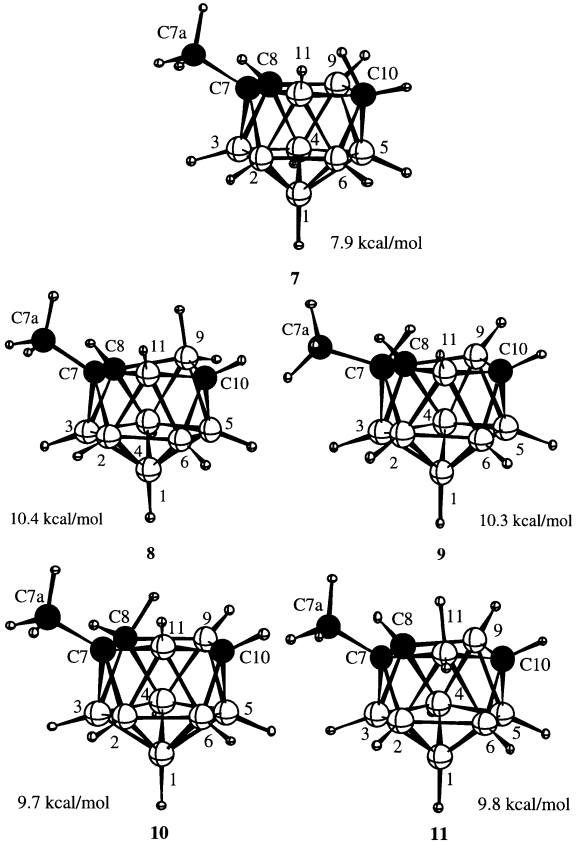

FIG. 3

Optimized geometries for possible structures for 7-Me-*nido*-7,8,10-$C_3B_8H_{11}$ (**7**–**11**). Relative energies (kcal/mol) for each structure optimized at B3LYP/6-311G* are relative to structure **14** (Fig. 4). Energies (kcal/mol): **7** (–225 890.9); **8** (–225 888.3); **9** (–225 888.5); **10** (–225 981.4); **11** (–225 888.9)

While cage-carbons are known to strongly favor the lower-coordinate positons on the open faces of carborane clusters, bridge-hydrogen placement can effect the carbon site preferences[26,27]. In some cases, carbons have been shown to adopt less-favorable higher-coordinate positions in the cage to allow a proton to adopt a favorable bonding configuration at a facial boron–boron edge. For example, the substituted derivatives of the eleven-vertex dicarbaborane anion [8-R-7,9-R′$_2$-*nido*-7,9-$C_2B_9H_9$]$^-$ (**12**) (where R = Me or $PhCH_2$; R′ = Me or H) lack a boron–boron edge to serve as a binding site for an additional proton; however, upon acidification they have been shown to rearrange, with one carbon moving from a lower-coordinate vertex on the open face to a higher-coordinate vertex in the belt below the open face, to yield the 11-R-2,7-R′$_2$-*nido*-2,7-$C_2B_9H_{10}$ (**13**) dicarbaborane containing a CB_4-face (Scheme 4). This rearrangement thus provides suitable B–B edges for a new bridging proton[28–31].

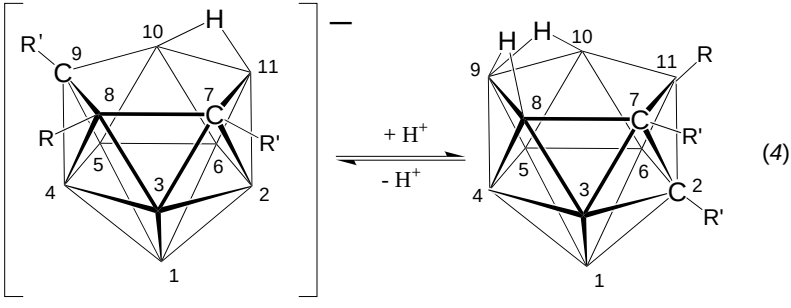

(*4*)

[8-R-7,9-R′$_2$-*nido*-7,9-$C_2B_9H_9$]$^-$ **12**

11-R-2,7-R′$_2$-*nido*-2,7-$C_2B_9H_{10}$ **13**

SCHEME 4

A similar type of carbon-rearrangement during the protonation reactions of **1a** and **1b** could also have the effect of generating a new B–B edge needed to better accommodate a proton. Therefore, other structures in which not all carbons are located on the open face were computationally examined for **2a** and **2b**. The boron and carbon chemical shifts of two isomers, 2-Me-*nido*-2,7,10-$C_3B_8H_{11}$ (**14**) and 7-Me-*nido*-3,7,9-$C_3B_8H_{11}$ (**15**) (Fig. 4), were found to be in good agreement with the experimental NMR chemical shifts (Table III). Significantly, both structures **14** and **15** have a lower relative energy at the DFT B3LYP/6-311G* level than any of the 7,8,10-structures (**7**–**11**) containing endo hydrogens. The GIAO calculated ^{11}B chemical shifts for the lowest energy structure **14**, in fact, show the best agreement with those experimentally determined for **2b** (Table III). Like-

wise, the calculated resonance assignments agree with the experimental measurements. For example, the resonances near –18 and –21 ppm, which were observed to have bridge-hydrogen coupling in the experimental 1D ^{11}B NMR spectra and in a 2D ^{11}B-^{1}H HETCOR experiment for **2a** and **2b**, are correctly predicted to be the hydrogen-bridged B8 and B9 borons in the calculated structure. Similarly, the other assignments experimentally determined by 2D ^{11}B-^{11}B COSY experiments, as well as the ^{13}C chemical shifts and assignments, match those of the calculations (Table III). Thus, the structure proposed for **2a** and **2b** is confirmed by the combined spectroscopic and computational studies as structure **14** (Fig. 4).

TABLE III
Comparison of the experimental ^{11}B and ^{13}C NMR chemical shifts and assignments of 2-R-*nido*-2,7,10-$C_3B_8H_{11}$ (**2a** and **2b**) with the calculated[a] shifts and assignments of structures: 2-Me-*nido*-2,7,10-$C_3B_8H_{11}$ (**14**) and 7-Me-*nido*-3,7,9-$C_3B_8H_{11}$ (**15**) (structures shown in Fig. 4)

2a Experimental	**2b** Experimental	**14** Calculated	**15** Calculated
	^{11}B NMR shifts		
–1.8 (B3)	0.73 (B3)	–0.58 (B3)	1.6 (B2)
–3.0 (B11)	–2.0 (B11)	–2.3 (B11)	–5.1 (B8)
–4.0 (B5)	–3.5 (B5)	–2.5 (B5)	–6.4 (B9)
–17.4 (B9)	–18.0 (B9)	–19.1 (B9)	–16.2 (B10)
–21.3 (B6)	–20.5 (B6)	–21.9 (B6)	–22.1 (B4)
–21.7 (B8)	–21.3 (B8)	–23.4 (B8)	–23.2 (B11)
–33.7 (B4)	–32.9 (B4)	–33.9 (B4)	–33.7 (B6)
–34.7 (B1)	–34.0 (B1)	–36.1 (B1)	–38.0 (B1)
	^{13}C NMR shifts		
57.8 (C2)	61.6 (C2)	60.60 (C2)	51.97 (C7)
36.8 (C10)	40.0 (C7)	42.97 (C7)	51.65 (C3)
33.0 (C7)	33.8 (C10)	38.85 (C10)	36.91 (C9)
[b]	23.3 (C2a)	25.71 (C2a)	25.20 (C7a)

[a] Calculations at the DFT B3LYP/6-311G*//B3LYP/6-311G* level; [b] benzyl carbon shifts not shown here, see Table I.

Deprotonation of the new 2-R-*nido*-2,7,10-$C_3B_8H_{11}$ (**2a** or **2b**) tricarbaboranes, without cage-rearrangement, would result in the formation of a new [2-R-*nido*-2,7,10-$C_3B_8H_{10}]^-$ (**3b**) tricarbollide anion (Scheme 5).

The DFT/GIAO calculated ^{11}B NMR shifts for such a new isomer (**3b**, structure **18** in Fig. 5) are given in Table IV. However, when **2a** and **2b** were

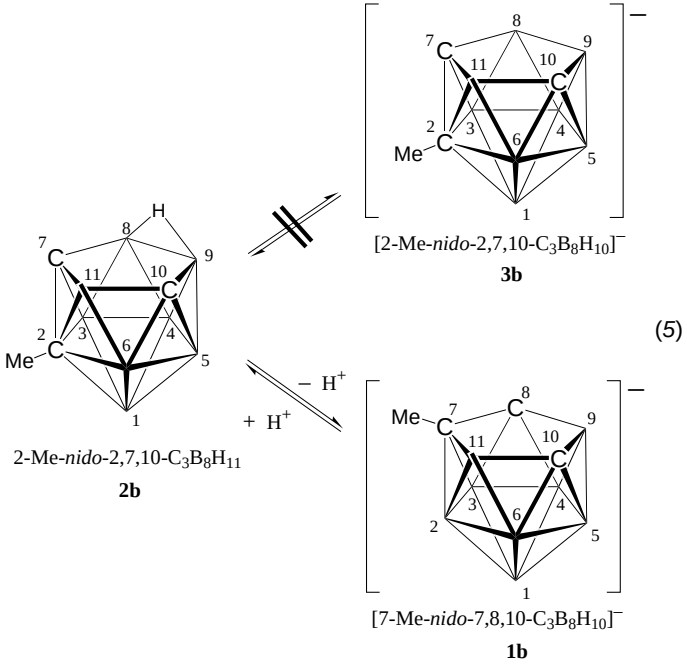

SCHEME 5

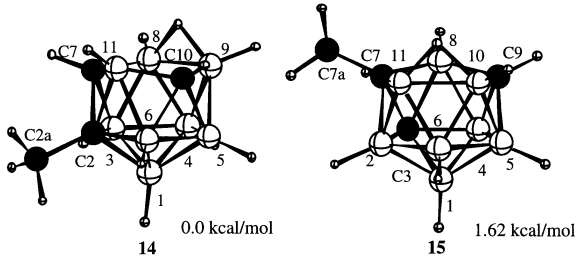

FIG. 4

Optimized geometries for **14** and **15**. Relative energies (kcal/mol) for each structure optimized at B3LYP/6-311G* are relative to structure **14**. Energies (kcal/mol): **14** (–225 898.8); **15** (–225 897.1)

deprotonated with proton sponge, the ^{11}B and ^{1}H NMR spectra of the resulting tricarbollide monoanions were identical to those of **1a** and **1b**. Their [7-R-*nido*-7,8,10-$C_3B_8H_{10}$]$^-$ structural assignment is again confirmed by the DFT/GIAO calculations which show excellent agreement between the calculated shifts and assignments for structure **16** and those experimentally determined for **1a** and **1b**. Thus, upon deprotonation the 2,7,10-skeletal rearrangement observed after protonation was reversed and the carbon atom in the five-coordinate two-vertex position in the neutral tricarbaboranes returns to the open face of the anions to give the 7,8,10-configuration. This result would indicate that while the 2,7,10-configuration is most stable for the neutral tricarbaborane, the

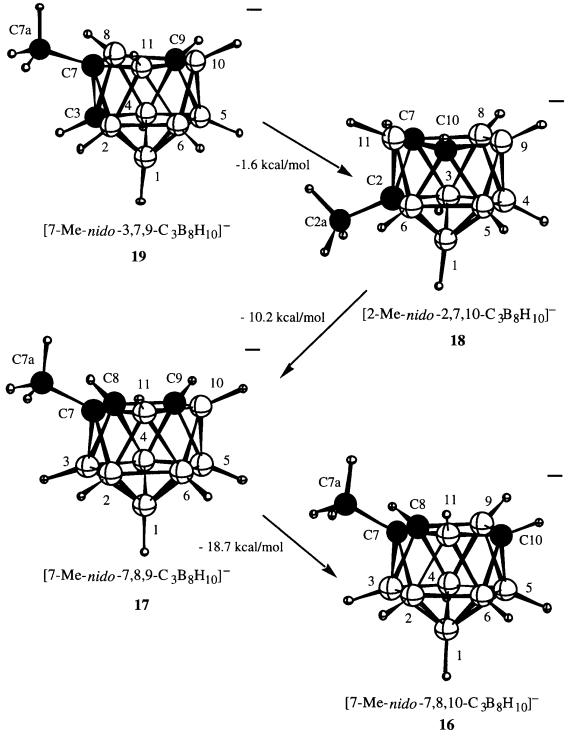

FIG. 5

Energy comparison of the DFT B3LYP/6-311G* optimized cage geometries for the four eleven-vertex *nido*-tricarbollide anions: [7-Me-*nido*-7,8,10-$C_3B_8H_{10}$]$^-$ (**16**), [7-Me-7,8,9-*nido*-$C_3B_8H_{10}$]$^-$ (**17**), [2-Me-*nido*-2,7,10-$C_3B_8H_{10}$]$^-$ (**18**), and [7-Me-*nido*-3,7,9-$C_3B_8H_{10}$]$^-$ (**19**). Energies (kcal/mol): **16** (–225 583.5); **17** (–225 564.8); **18** (–225 439.7); **19** (–225 553.0)

7,8,10-configuration is the most stable for the anions. This conclusion was confirmed by DFT and DFT/GIAO calculations[32] on four possible tricarbollide anion structures (**16**–**19**) (Fig. 5, Table IV).

The calculations show that the [7-Me-*nido*-7,8,10-$C_3B_8H_{10}$]$^-$ tricarbollide anion (**16**) is the most stable of the four isomers. It is 18.7 kcal/mol lower in energy than the adjacent carbon [7-Me-*nido*-7,8,9-$C_3B_8H_{10}$]$^-$ isomer (**17**) (Fig. 5). This agrees with Schleyer's previous calculation that the parent isomer, [*nido*-7,8,10-$C_3B_8H_{11}$]$^-$, is 18.3 kcal/mol more stable than [*nido*-7,8,9-$C_3B_8H_{11}$]$^-$ at the MP2/6-31G* level of optimization[14] and likewise, is consistent with the report that thermolysis of Cs^+[*nido*-7,8,9-$C_3B_8H_{11}$]$^-$ at 350 °C resulted in the formation of Cs^+[*nido*-7,8,10-$C_3B_8H_{11}$]$^-$ (63% yield)[12,14].

TABLE IV

Comparison of the calculated[a] and experimental ^{11}B and ^{13}C NMR assignments and shifts for [*nido*-$MeC_3B_8H_{10}$]$^-$ tricarbollide anion isomers: [7-Me-*nido*-7,8,10-$C_3B_8H_{10}$]$^-$ (**16**), [7-Me-7,8,9-*nido*-$C_3B_8H_{10}$]$^-$ (**17**), [2-Me-*nido*-2,7,10-$C_3B_8H_{10}$]$^-$ (**18**), and [7-Me-*nido*-3,7,9-$C_3B_8H_{10}$]$^-$ (**19**) (structures shown in Fig. 5)

1b Experimental	**16** Calculated	**17** Calculated	**18** Calculated	**19** Calculated
		^{11}B NMR shifts		
–11.6 (B3)	–11.6 (B3)	–14.4 (B6)	–14.4 (B3)	–10.6 (B10)
–17.2 (B11)	–18.2 (B6)	–16.5 (B11)	–15.3 (B9)	–13.3 (B2)
–18.5 (B6)	–19.1 (B11)	–17.1 (B2)	–17.6 (B11)	–21.5 (B6)
–19.0 (B9)	–20.2 (B9)	–17.8 (B10)	–18.5 (B5)	–21.9 (B8)
–21.5 (B5,2)	–20.9 (B5)	–21.2 (B3)	–21.9 (B4)	–22.7 (B5)
	–22.5 (B2)	–23.8 (B5)	–23.5 (B8)	–24.0 (B11)
–25.4 (B4)	–26.3 (B4)	–25.1 (B4)	–23.6 (B6)	–24.4 (B4)
–48.0 (B1)	–49.7 (B1)	–48.6 (B1)	–53.1 (B1)	–54.4 (B1)
		^{13}C NMR shifts		
[b]	45.06 (C7)	50.53 (C7)	44.48 (C2)	44.16 (C7)
35.8 (C8)	36.79 (C8)	40.15 (C8)	35.4 (C7)	42.41 (C7)
27.66 (C10)	31.99 (C10)	36.63 (C9)	28.63 (C2a)	26.52 (C7a)
24.10 (C7a)	25.93 (C7a)	27.68 (C10)	27.68 (C10)	26.23 (C9)

[a] Calculations at the DFT B3LYP/6-311G*//B3LYP/6-311G* level; [b] not observed at room temperature.

The other two isomers, **18** and **19**, in which one of the cage carbons is no longer present on the open face, are close in energy (1.6 kcal/mol energy difference), but are ≈29 kcal/mol higher in energy than **16**. This result is in agreement with the fact that one carbon in both **18** and **19** is now located in an unfavorable penta-coordinate position. Structure **18** (2-Me-2,7,10-), containing one penta-coordinate carbon and two tetra-coordinate carbons, is less stable by 28.9 kcal/mol than **16** (7-Me-7,8,10-), where all three carbons are tetra-coordinate (Fig. 5), again demonstrating the strong carbon preference for low-coordinate cage sites[33,34].

Thus, deprotonation of **2b** (*nido*-2-Me-2,7,10-$C_3B_8H_{11}$) results in cage rearrangement back to the starting tricarbollide monoanion geometry, [*nido*-7-Me-7,8,10-$C_3B_8H_{10}$]$^-$ (**1b**). At first glance, the mechanism of the interconversion of the 7,8,10- and 2,7,10-framework would seem to be complex and require several simultaneous atom movements within the framework. However, as shown in Scheme 6, this rearrangement does not require a "carbon-migration", but instead can be accomplished by a simple, straightforward process that requires the movement of only one cage atom, B11, from its original position in the C7–B8–B9–C10–B11 plane of the 2,7,10-anion (**3b**) to the B9-position in the C7–C8–B9–C10–B11 plane of the 7,8,10-anion **1b**.

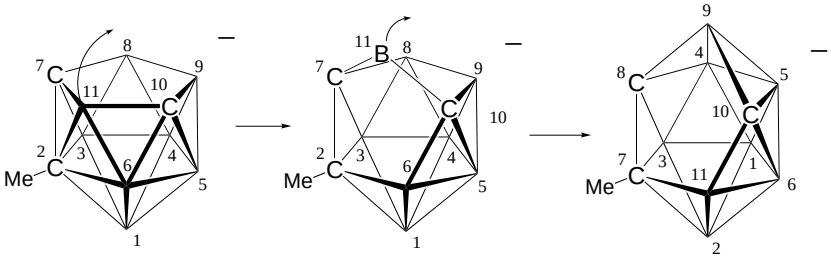

SCHEME 6

Transition state calculations at the HF/6-31G*-level, in fact, yielded a low-energy (activation barrier of only 6.5 kcal/mol) pathway (Fig. 6) for the rearrangement of [2-Me-*nido*-2,7,10-$C_3B_8H_{10}$]$^-$ (**3b**, structure **18**) to [7-Me-*nido*-7,8,10-$C_3B_8H_{10}$]$^-$ (**1b**, structure **16**) that is consistent with the process outlined in Scheme 6. A true transition state (**TS18/16**) was located that has a structure in which the B11 atom is rotated into a double-coordinate position 24° out of the C7–B8–B9–C10 plane and only 36.5° from the C2–C7–C10–B6 plane of **3b**. Likewise, in the **TS18/16** structure,

the B11–B6 and B11–C2 distances are lengthened out of normal bonding ranges (B11–B6: from 1.856 to 2.164 Å; B11–C10: from 1.797 to 2.209 Å), and the B11–B8 and B11–B9 distances are slightly decreased (B11–B8: from 2.662 to 2.564 Å; B11–B9: from 2.653 to 2.522 Å) compared to those found in **1b**. A continued rotation of the B11 atom in the **TS18/16** structure (Fig. 6) in the manner depicted in Scheme 6 would then yield the lower energy structure [7-Me-*nido*-7,8,10-$C_3B_8H_{10}$]$^-$ structure observed for **1b**.

In conclusion, protonation of the tricarbollide anions, [7-R-*nido*-7,8,10-$C_3B_8H_{10}$]$^-$ (where R = $PhCH_2$ (**1a**) or R = Me (**1b**)), results in the formation of the new eleven-vertex tricarbaboranes, 2-R-*nido*-2,7,10-$C_3B_8H_{11}$ (where R = $PhCH_2$ (**2a**) or R = Me (**2b**)) in which one cage-carbon adopts an unfavorable higher-coordinate skeletal-position. The process is apparently driven by the need to generate a favorable B–B bonding-edge for the incoming proton. These results again demonstrate that either carbon-site or hydrogen-placement preferences can be the dominate factor in determining cage-geometry. The fact that the process is reversible and proceeds readily is consistent with the proposed low-energy pathway involving the movement of only one-facial atom. These results also suggest that such a mechanism

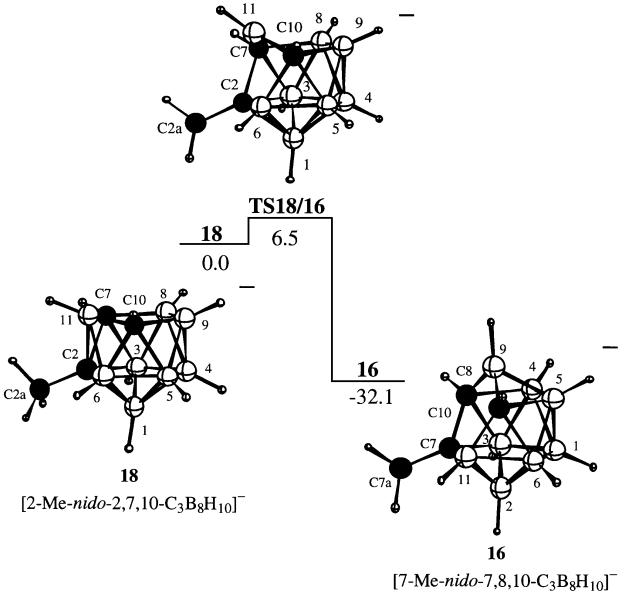

FIG. 6

Potential energy diagram. Stationary points with relative energies (kcal/mol), optimized at HF/6-31G*, along the schematic reaction path

may be involved in similar rearrangements that have been observed in related cage systems, such as in the protonation–isomerization reaction leading to the conversion of [8-R-7,9-R'_2-*nido*-7,9-$C_2B_9H_9$]$^-$ (**12**) to 11-R-2,7-R'_2-*nido*-2,7-$C_2B_9H_{10}$ (**13**). We are presently exploring these possibilities.

We thank the National Science Foundation for the support of this research. We also thank Prof. J. Bausch for his advice on reaction pathway calculations.

REFERENCES AND NOTES

1. Su K., Barnum B. A., Carroll P. J., Sneddon L. G.: *J. Am. Chem. Soc.* **1992**, *114*, 2730.
2. Plumb C. A., Carroll P. J., Sneddon L. G.: *Organometallics* **1992**, *11*, 1665.
3. Plumb C. A., Carroll P. J., Sneddon L. G.: *Organometallics* **1992**, *11*, 1672.
4. Plumb C. A., Sneddon L. G.: *Organometallics* **1992**, *11*, 1681.
5. Su K., Carroll P. J., Sneddon L. G.: *J. Am. Chem. Soc.* **1993**, *115*, 10004.
6. Shedlow A. M., Carroll P. J., Sneddon L. G.: *Organometallics* **1995**, *14*, 4046.
7. Weinmann W., Wolf A., Pritzkow H., Siebert W., Barnum B. A., Carroll P. J., Sneddon L. G.: *Organometallics* **1995**, *14*, 1911.
8. Štíbr B., Holub J., Teixidor F., Viñas C.: *Collect. Czech. Chem. Commun.* **1995**, *60*, 2023.
9. Štíbr B., Holub J., Teixidor F., Viñas C.: *J. Chem. Soc., Chem. Commun.* **1995**, 795.
10. Barnum B. A., Carroll P. J., Sneddon L. G.: *Organometallics* **1996**, *15*, 645.
11. Štíbr B., Holub J., Císařová I., Teixidor F., Viñas C., Fusek J., Plzák Z.: *Inorg. Chem.* **1996**, *35*, 3635.
12. Štíbr B., Holub J., Císařová I., Teixidor F., Viñas C.: *Inorg. Chim. Acta* **1996**, *245*, 129.
13. Rousseau R., Lee S., Canadell E., Teixidor F., Viñas C., Štíbr B.: *New J. Chem.* **1996**, *20*, 277.
14. Holub J., Štíbr B., Hynk D., Fusek J., Císařová I., Teixidor F., Viñas C., Plzák Z., Schleyer P. v. R.: *J. Am. Chem. Soc.* **1997**, *119*, 7750.
15. Barnum B. A., Carroll P. J., Sneddon L. G.: *Inorg. Chem.* **1997**, *36*, 1327.
16. Wille A. E., Sneddon L. G.: *Collect. Czech. Chem. Commun.* **1997**, *62*, 1214.
17. Wasczcak M. D., Hall I. H., Carroll P. J., Sneddon L. G.: *Angew. Chem., Int. Ed. Engl.* **1997**, *36*, 2228.
18. Shriver D. F., Drezdzon M. A.: *Manipulation of Air Sensitive Compounds*, 2nd ed. Wiley, New York 1986.
19. Kang S. O., Carroll P. J., Sneddon L. G.: *Organometallics* **1988**, *7*, 772.
20. Yang X., Jiao H., Schleyer P. v. R.: *Inorg. Chem.* **1997**, *36*, 4897; and references therein.
21. Frisch M. J., Trucks G. W., Schlegel H. B., Gill P. M. W., Johnson B. G., Robb M. A., Cheeseman J. R., Keith T., Petersson G. A., Montgomery J. A., Raghavachari K., Al-Laham M. A., Zakrzewski V. G., Ortiz J. V., Foresman J. B., Cioslowski J., Stefanov B. B., Nanayakkara A., Challacombe M., Peng C. Y., Ayala P. T., Chen W., Wong M. W., Andres J. L., Replogle E. S., Gomperts R., Martin R. L., Fox D. J., Binkley J. S., Defrees D. J., Baker J., Stewart J. P., Head-Gordon M., Gonzalez C., Pople J. A.: *Gaussian 94, Revision C.3*. Gaussian, Inc., Pittsburgh (PA) 1995.
22. Shedlow A. M., Sneddon L. G.: *Inorg. Chem.* **1998**, *37*, 5269.
23. Tebben A. J.: *M. Thesis*. Villanova University, Villanova (PA) 1997.

24. Tebben A. J., Bausch J. W.: Unpublished results.
25. Transition state optimization using the Synchronous Transit-Guided Quasi-Newton (STQN) Method utilized the QST3 option in which three molecule specifications were provided: the reactants, the products and an initial transition state structure.
26. Tebben A. J., Ji G., Williams R. E., Bausch J. W.: *Inorg. Chem.* **1998**, *37*, 2189.
27. Williams R. E.: *Chem. Rev.* **1992**, *92*, 117.
28. Zakharkin L. I., Zhigareva G. G., Antonovich V. A., Yanovskii A. I., Struchkov Y. T.: *Bull. Acad. Sci. USSR, Div. Chem. Sci.* **1984**, 1534.
29. Knyazev S. P., Bratsev V. A., Stanko V. I.: *Dokl. Akad. Nauk SSSR, Ser. Khim.* **1977**, *234*, 1093.
30. Onak T. in: *Comprehensive Organometallic Chemistry* (G. Wilkinson, F. G. A. Stone and E. W. Abel, Eds), Vol. 1, p. 438. Pergamon Press, New York 1982.
31. Štíbr B.: *Chem. Rev.* **1992**, *92*, 225.
32. The ^{11}B chemical shifts and assignments for the tricarbollide anion, [7-Me-*nido*-7,8,10-$C_3B_8H_{10}]^-$, have previously been reported at the HF/6-31G* level of optimization. See ref.[6].
33. Williams R. E.: *Inorg. Chem.* **1971**, *10*, 210.
34. Bausch J. W., Rizzo R. C., Sneddon L. G., Wille A. E., Williams R. E.: *Inorg. Chem.* **1996**, *35*, 131.